Effect of Cholesterol and Ergosterol on the Compressibility and Volume Fluctuations of Phospholipid-Sterol Bilayers in the Critical Point Region: A Molecular Acoustic and Calorimetric Study

Roland Krivanek, Linus Okoro, and Roland Winter
University of Dortmund, Department of Chemistry, Physical Chemistry I – Biophysical Chemistry, Dortmund, Germany

ABSTRACT Although sterol-phospholipid interactions have been of interest for many years now, a complete thermodynamic profile of these systems is still missing. To contribute to a better understanding of the thermodynamic functions of these systems, we determined isothermal compressibility coefficient data for dipalmitoylphosphocholine (DPPC) and DPPC-containing cholesterol and ergosterol vesicles by means of molecular acoustics (ultrasound velocimetry and densimetry) and differential scanning and pressure perturbation calorimetric techniques. A particular focus was on the influence of the differential structural properties of the two sterols on the thermodynamic properties of lipid bilayers, and on the nature of the critical point region of phospholipid-sterol systems by determining thermodynamic fluctuation parameters. Contrary to significant changes in conformational and dynamical properties of the DPPC-sterol membranes, no marked differences were found in the various thermodynamic properties studied, including the adiabatic (β_S^{lipid}) and isothermal (β_T^{lipid}) compressibility, as well as the volume fluctuations. Differences in β_T^{lipid} and β_S^{lipid} become dramatic in the gel-fluid transition region only, due to a significant degree of slow relaxational processes in the microsecond time range in the transition region. Our data show no evidence for the existence of a typical critical point phenomenon in the concentration and temperature range where a critical point in the DPPC-sterol phase diagram is expected to appear. Hence, on a macroscopic level, it seems more appropriate to describe the sterol-phospholipid binary mixtures in the liquid-ordered/liquid-disordered coexistence region as a phase region consisting essentially of small nanodomains only. Such small-domain dimensions, with a series of particular properties such as increased line energy, spontaneous curvature, and limited lifetime, seem also to be typical of raftlike domains in cell membranes.

INTRODUCTION

Sterols are essential components of eukaryotic cells both as structural membrane components and as initiators and regulators of biological processes (1–4). In particular, cholesterol (Chol) is ubiquitous in mammalian cells and ergosterol (Erg) is the major sterol in many fungi and protozoans. These sterols fulfill various functions, including growth stimulation and regulating and maintaining membrane elasticity, permeability, and integrity. However, details of the interaction of sterols with lipid membranes and differential properties of the various sterols are still a matter of controversy, despite enormous efforts dedicated to this issue over several decades (1–21).

It is widely accepted that cholesterol can induce a liquid-ordered (l_o) state in lipid bilayer membranes, which has intermediate properties between a gel phase (ordered acyl chains) and a liquid-disordered (l_d), fluidlike phase with high lateral mobility (4,22,23). A macroscopic separation of two liquid (l_o and l_d) phases has been observed for ternary mixtures of, e.g., 1,2-dioleoyl-*sn*-glycero-3-phosphocholine (DOPC), 1,2-dipalmitoyl-*sn*-glycero-3-phosphocholine (DPPC), and cholesterol (22,24,25). There is, however, an ongoing debate as to whether also binary lipid mixtures are best described assuming $l_o + l_d$ macroscopic coexistence in a certain composition and temperature range (see, e.g., (5,26–28)). A variety of detailed experimental studies led to a widely accepted phospholipid-cholesterol/ergosterol phase diagram (6,13,14, 19,29,30), indicating that the amphiphilic compounds cholesterol and ergosterol are able to induce both ordered and disordered fluid phases in a phospholipid bilayer. As cholesterol interacts differently with the translational and the conformational degrees of freedom of the phospholipid molecules, a liquid-ordered phase (29) has been postulated to exist at cholesterol contents >20 mol %. Though it exhibits a high degree of conformational order, this phase lacks translational order.

In Fig. 1, the experimentally proposed but still intensively discussed phase diagrams of the DPPC-Chol binary mixture (*open circles*) (13) and that of DPPC-Erg (*solid circles*) (6) are presented. The one-phase—l_d, s_o, and l_o—and two-phase—$s_o + l_o$ and $l_d + l_o$—regions are shown. Here, T_m is the gel-to-fluid melting temperature of the pure lipid compound (T_m = 41.5°C for DPPC). The $l_d + l_o$ two-phase regions seem to end in a critical point at concentration ~20–24 mol % sterol, in a concentration region where the distinction between liquid-disordered and liquid-ordered phases disappears at high temperatures. The exact location and character of the critical point region is still under debate, however.

It is of interest to note that Xu et al. (27) found that ergosterol promotes the formation of raftlike domains more

Submitted September 22, 2007, and accepted for publication December 20, 2007.

Address reprint requests to Roland Winter, University of Dortmund, Department of Chemistry, Physical Chemistry I – Biophysical Chemistry, Otto-Hahn-Straße 6, D-44227 Dortmund, Germany. Tel.: 49-231-755-3900; Fax: 49-231-755-3901; E-mail: roland.winter@uni-dortmund.de.

Editor: Enrico Gratton.

0006-3495/08/05/3538/11 $2.00

doi: 10.1529/biophysj.107.122549

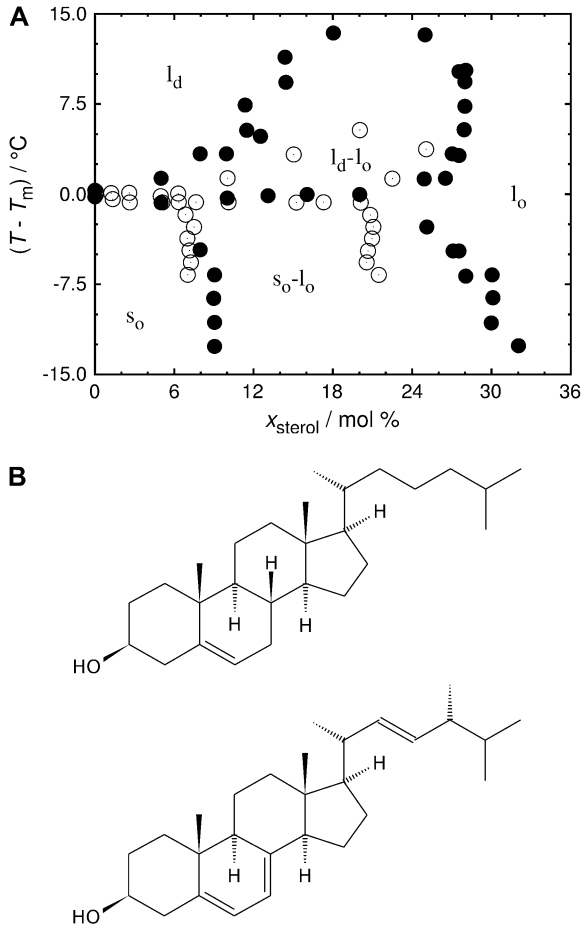

FIGURE 1 (*A*) Experimentally proposed phase diagrams of the DPPC-Chol binary mixture, adopted from Vist and Davis (13) (*open circles*) and that of DPPC-Erg, adopted from Hsueh et al. (6) (*solid circles*). s_o, solid-ordered lipid phase; l_d, liquid-disordered lipid phase; l_o, liquid-ordered lipid phase. (*B*) Chemical structure of cholesterol (*upper*) and ergosterol (*lower*).

strongly than cholesterol does. Indeed, Urbina et al. (31) have shown that, compared with cholesterol, 30 mol % ergosterol orders the acyl chains of 1,2-dimyristoyl-3-*sn*-phosphatidylcholine (DMPC) more strongly. Endress et al. (32) compared the effects of cholesterol and ergosterol on the mechanical properties of DPPC bilayers. They found that the area compressibility modulus of DPPC bilayers containing 40 mol % ergosterol at 10°C is a factor of 1.5 higher than in the case of cholesterol. Small-angle neutron scattering on DMPC with 20 and 47 mol % sterol mixtures by Pencer et al. (33) revealed a lower compressibility of ergosterol compared to cholesterol, i.e., that ergosterol has a greater condensing effect. Tierney et al. (14) revealed a similar condensation effect of both sterols at a concentration level of 40 mol % for DPPC-sterol mixtures. Bacia et al. (9) also showed that a different sterol structure may induce a different curvature of giant unilamellar vesicles of model raft mixtures. Recently, we investigated the influence of the sterol side chain and ring structure on the acyl chain orientational order of lipid bilayers by measuring the steady-state fluorescence anisotropy of the fluorophore 1-(4-trimethylammonium-phenyl)-6-phenyl-1,3,5-hexatriene (TMA-DPH) to establish the molecular basis underlying the changes in order parameter of the lipid bilayer system (21). Sterols with the bulkiest unsaturated side chains or sterol nuclei (stigmasterol, β-sitosterol, and lanosterol) induce the smallest order parameter increase of the fluid bilayer at high sterol concentrations (>30 mol %) and hence become less potent rigidifiers at high sterol levels. At the highest sterol levels, cholesterol and–even more pronouncedly—the plant sterol ergosterol have the most profound ordering effect on fluid DPPC bilayers (21).

In this study, to reveal further differences in properties of sterols in lipid bilayers, we studied new thermodynamic properties of dispersions of DPPC with cholesterol and ergosterol. In addition to differential scanning calorimetric (DSC) and pressure perturbation calorimetric (PPC) measurements, measurements of ultrasonic velocity and density were carried out to determine the adiabatic and isothermal compressibilities, as well as to yield information about the volume fluctuations of the systems. Until now, generally only the adiabatic compressibility of lipid systems has been determined. However, to study critical phenomena, the isothermal compressibility is required, which is directly proportional to the volume fluctuations of the system. The difference is most pronounced in the gel-fluid phase transition region due to the relaxation slowing down, where the adiabatic compressibility is not able to capture slow processes.

Significant thermodynamic fluctuations are known to exist near the gel-to-fluid chain-melting phase transition of pure lipid bilayers. They occur over a narrow, but finite, temperature range, in which the heat capacity at constant pressure displays a rather sharp maximum and other physical membrane properties, such as the specific volume, reveal rather sharp or steplike changes, indicating a first-order transition (34,35). The heat capacity and compressibility are related to fluctuations in enthalpy and volume, respectively (36–38). The amplitude of the fluctuations increases when approaching the phase transition, as is characteristic for a second-order transition. Obviously, the build-up of fluctuations would lead to a critical point if not preceded by the first-order transition. Therefore, the gel-to-fluid membrane transition is usually considered weak first-order (39,40). In this study, we focused also on the fluid-fluid critical point region of DPPC-sterol mixtures to reveal the importance of fluctuations in the $l_o + l_d$ critical point region and hence to gain information about the nature of the transition in these systems.

MATERIALS AND METHODS

Sample preparation

1,2-Dipalmitoyl-3-*sn*-phosphatidylcholine (DPPC) was purchased from Avanti Polar Lipids (Alabaster, AL). Ergosterol and cholesterol were obtained from Fluka (Taufkirchen, Germany) and SIGMA (Deisenhofen, Germany), respectively. Both DPPC and sterols were used without further purification. To produce DPPC-sterol mixtures, lipids were dissolved in an

organic solvent (chloroform/methanol 3:1 v/v mixture) and mixed in appropriate ratios. The solvent was afterwards removed with a gentle nitrogen steam so that the lipid formed a thin layer on the wall of the tube. The remainders of the solvent were subsequently removed in a freeze-dryer (Christ, Osterode, Germany) under high vacuum overnight. A Tris buffer (10 mM Tris, pH 7.4, with 100 mM NaCl) was used to hydrate dried lipid mixtures by vortexing at ~62°C (above the main phase transition temperature, T_m, of DPPC (~41.5°C) (41)), resulting in homogeneous multilamellar vesicles (MLVs). For the calorimetric measurements, the obtained MLVs were sonicated for 30 min at a temperature above T_m and subjected to six freeze/thaw cycles. Large unilamellar vesicles (LUVs) of uniform shape and size used in the ultrasound velocity and the density measurements were prepared from the MLVs by extrusion (42) using a Mini-Extruder (Avanti Polar Lipids, Alabaster, AL), and passing them through 100 nm Nuclepore Polycarbonate Track-Etch Membranes (Whatman, Dassel, Germany) at ~62°C. The final DPPC concentration used in the ultrasound velocity and density measurements was 5 mg/mL, and in the calorimetric measurements 20 mg/mL.

Ultrasound velocity and density measurements

The speed of sound propagation in a medium, u, the density, ρ, and the adiabatic compressibility coefficient, $\beta_S = -1/V(\partial V/\partial p)_S$ (where V, p, and S are the volume, pressure, and entropy, respectively) are coupled to each other by the relationship

$$\beta_S = 1/u^2\rho. \quad (1)$$

This method can also be applied to solutions of biomolecules in water, such as lipid dispersions. The ultrasound velocity measurements were performed with a commercial differential ultrasonic resonator device ResoScan (TF Instruments, Heidelberg, Germany (43,44)) operating in a frequency range of 7.2–8.5 MHz. The sound velocity in the lipid dispersion was determined relative to that in the buffer solution at the same temperature in terms of the velocity number, $[u]$, defined as (45)

$$[u] = (u - u_0)/u_0 c, \quad (2)$$

where u and u_0 denote the sound velocity in the solution and solvent, respectively, and c (in mol/L) is the solute concentration.

A high-precision density meter, DMA 5000 (Anton Paar, Graz, Austria), based on the mechanical oscillator principle (46), corrected for viscosity-induced errors, was employed to measure the densities, ρ and ρ_0, of the lipid solution and the solvent, respectively, which were further used for the evaluation of the partial molar volume, V^o, of the lipid according to

$$V^o = \left(\frac{\partial V}{\partial n}\right) \cong \frac{M}{\rho_0} - \frac{\rho - \rho_0}{\rho_0 c}, \quad (3)$$

where V is the volume, n the number of solute molecules in moles, and M is the molar mass of the solute. It must be noted that the approximation is valid only for diluted lipid suspensions, as used here.

In molecular acoustics, due to the additivity of all components of the system, the partial molar adiabatic compressibility, K_S^o, is generally used, given by

$$K_S^o = \left(\frac{\partial K_S}{\partial n}\right) = \left(\frac{\partial V^o}{\partial p}\right)_S \cong \beta_{S,0}\left(2(V^o - [u]) - \frac{M}{\rho_0}\right), \quad (4)$$

where $K_S = \beta_S V$ is the adiabatic compressibility and $\beta_{S,0}$ is the adiabatic compressibility coefficient of the solvent. Here again, as in the case of the partial molar volume, the approximation is valid only for diluted lipid samples. By dividing the partial molar quantities V^o and K_S^o by the molar mass of the solute we obtain the partial specific values, i.e., the partial specific volume, v^o, and the partial specific adiabatic compressibility, k_S^o. Accordingly, the concentration, c, in Eq. 2 becomes c/M, which is then expressed in mg/mL.

The sound velocity was determined with a relative error better than 10^{-3}%, corresponding to a precision higher than 5×10^{-5} mL/g in $[u]$. The density values were measured with relative error $<10^{-3}$%, so the accuracy in v^o is better than 10^{-4} mL/g. Hence, considering the relative errors of $[u]$ and v^o, the certainty in k_S^o taken from Eq. 4 is within 10^{-12} mL/gPa. In both methods, the corresponding values were measured at discrete temperatures (read with an accuracy of 10^{-3}°C), resulting in an average temperature scan rate of ~12°C/h.

Calorimetric measurements

Differential scanning calorimetry (DSC) measurements were performed with a VP DSC calorimeter from MicroCal (Northampton, MA). The sample cell of the calorimeter was filled with ~0.5 mL of MLV lipid suspension with a DPPC concentration of 20 mg/mL, whereas the reference cell was filled with a corresponding buffer solution and hence, the excess heat capacities, ΔC_p, are given with respect to the reference.

Pressure perturbation calorimetry (PPC, (47–52)) measurements were performed on the same VP DSC calorimeter mentioned above equipped with MicroCal's PPC accessory pressurizing system (Northampton, MA). Bidirectional gas (N_2) pressure-jumps applied to the samples had an amplitude of 5 bar. Under the same experimental conditions, a set of sample-buffer, buffer-buffer, buffer-water, and water-water measurements was carried out each time to evaluate the thermal expansion coefficient of the lipid(s), α. The procedure was repeated automatically at many temperatures. Hence, the technique measures the heat response of the lipid to a very small pressure change at constant temperature, corresponding to the differential $(\partial Q/\partial p)_T$. This differential heat is related to the isobaric, thermal volume expansion, $(\partial V/\partial T)_p$, which can be seen by inserting the equation for the heat of a reversible process, $dS = dQ/T$, into the Maxwell relation for the isothermal entropy change with pressure, $(\partial S/\partial p)_T = -(\partial V/\partial T)_p$. The results can be expressed as the coefficient of thermal expansion, $\alpha = 1/V(\partial V/\partial T)_p$, at constant pressure. Since the partial specific volume of the mixed membrane varies only slightly (~2%, see results) compared to the pure DPPC bilayer, the partial specific volume of DPPC was used for the calculation of α. The effect on the resulting thermal expansion coefficient is negligible.

In both calorimetric techniques, a scan rate of 40°C/h was used.

RESULTS AND DISCUSSION

Calorimetric measurements on DPPC-sterol mixtures

Since a detailed discussion of the DSC and PPC data of the two systems investigated and of other sterol systems, are the topic of another article (L. Okoro and R. Winter, unpublished), as an example, we show the ergosterol data only. The cholesterol data are in good agreement with published results (8,10). Fig. 2 shows the DSC and PPC scans of the system DPPC-Erg. Pure DPPC displays the well-known sharp main transition (the s_o (or $P_{\beta'}$ gel)-to-l_d transition) near 41.5°C, and a smaller peak due to the $L_{\beta'}$-$P_{\beta'}$ pretransition, which appears at 35°C. In agreement with data from Hsueh et al. (6), at 5 mol % ergosterol, the main transition becomes broadened and shifts toward a lower temperature. The broad transition in the 5 mol % ergosterol membrane indicates a s_o and l_d phase coexistence region. As the ergosterol concentration increases to 22 mol %, the intensity of the main DSC peak decreases, and the peak position seems to remain essentially unchanged. A broad shoulder appears on the high-temperature side of the sharp peak, suggesting a (l_d + l_o) two-phase region (Fig. 1). Where the broad peak ends, the transition to the l_d phase

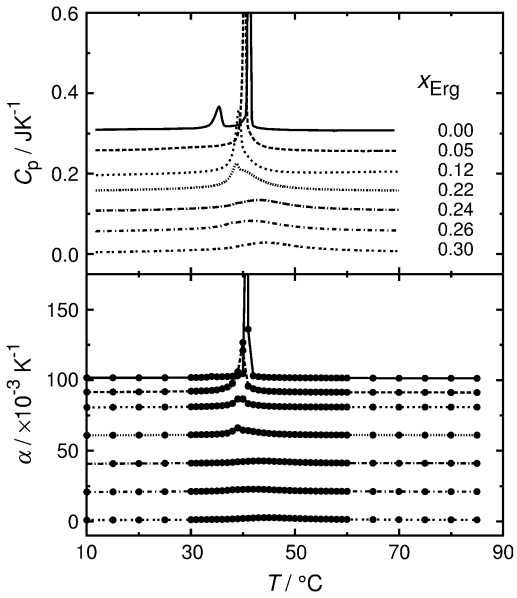

FIGURE 2 DSC (*upper*) and PPC (*lower*) scans of the DPPC-Erg system. The curves for ergosterol concentrations below 30 mol % are upward-shifted for better visibility.

occurs. At ergosterol concentrations of 30 mol % and above, only a very broad residual endotherm is observed, similar to that seen in DPPC-Chol MLVs.

Molecular acoustic measurements on DPPC-Chol and DPPC-ergosterol mixtures

Employing the sound velocity and density measurements, the velocity number, $[u]$, and the partial specific volume, v^o, of the DPPC-sterol mixtures were evaluated. Using Eq. 4 (adapted for partial specific volume values), the partial specific adiabatic compressibility, k_S^o, of the lipid suspensions was determined also. Figs. 3 and 4 show the temperature dependence of $[u]$ (*upper*), v^o (*middle*), and k_S^o (*lower*) for the binary DPPC-Chol and DPPC-Erg mixtures, respectively, at 0, 5, 12, 22, 24, 26, and 30 mol % of sterol, in the temperature range 5–85°C. In both cases, at points distant from the lipid main phase transition temperature, T_m, $[u]$ decreases as the temperature rises, whereas the typical pronounced anomalous dip (53–57) in the vicinity of T_m for pure lipid (*solid line*) and low sterol contents (both cholesterol and ergosterol at 5 and 12 mol %, represented by *long*- and *short-dashed lines*, respectively) of DPPC LUVs appears. The lowest value reached for $[u]$, −0.15 mL/g for pure DPPC vesicles around the T_m, is consistent with the data of Mitaku and co-workers (53), but is somewhat lower than the value of −0.12 mL/g found by Kharakoz et al. (54), and higher than that of −0.26 mL/g found by Schrader et al. (55). It must be noted, however, that the depth and width of the dip in $[u]$ depend on the sample preparation (53), which is related to the different degree of cooperativity of the main phase transition, the lipid concentration (54), and the ultrasound frequency applied for the

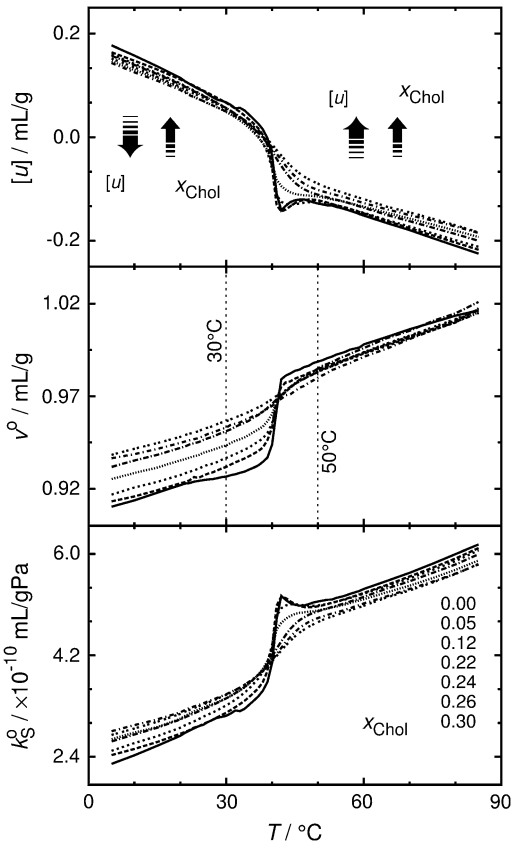

FIGURE 3 The temperature dependence of the ultrasound velocity number, $[u]$ (*upper*), the partial specific volume, v^o (*middle*), and the partial specific adiabatic compressibility, k_S^o (bottom), of DPPC-Chol mixtures at different cholesterol molar fractions, x_{Chol}. The arrows indicate the different effects of the increasing cholesterol content on $[u]$ bellow and above the phase transition temperature, T_m, of DPPC (41.5°C) (see text).

measurement itself (56), which is related to the heat exchange within the period of the sound wave (58,59). In addition, inadequately high temperature scan rates might induce a slight shift in the dip minimum position toward higher temperatures (60), since lipid bilayers are not able to thermally equilibrate rapidly due to molecular processes slowing down during the main phase transition.

At the proposed critical concentration of ~22 mol % sterol, $[u]$ still shows a weak minimum, which fully vanishes at higher sterol content (24, 26, and 30 mol %, represented by *long* and *short dash-dotted* and *dot-dotted lines*, respectively). This issue will be discussed in detail later in connection to the isothermal compressibility data. Outside the main phase transition region, in general, $[u]$ is smaller below T_m and larger above T_m for both DPPC-sterol mixtures than for pure DPPC LUVs, reflecting the different (disordering and ordering) effects of sterols on DPPC in the gel and liquid-crystalline phases, respectively (3,21,35,57). Conversely, v^o increases monotonously with temperature in the whole temperature range measured for both sterols. For pure DPPC and for the low sterol concentrations (5, 12, and 22 mol %), a steplike change around T_m is observed, which disappears at

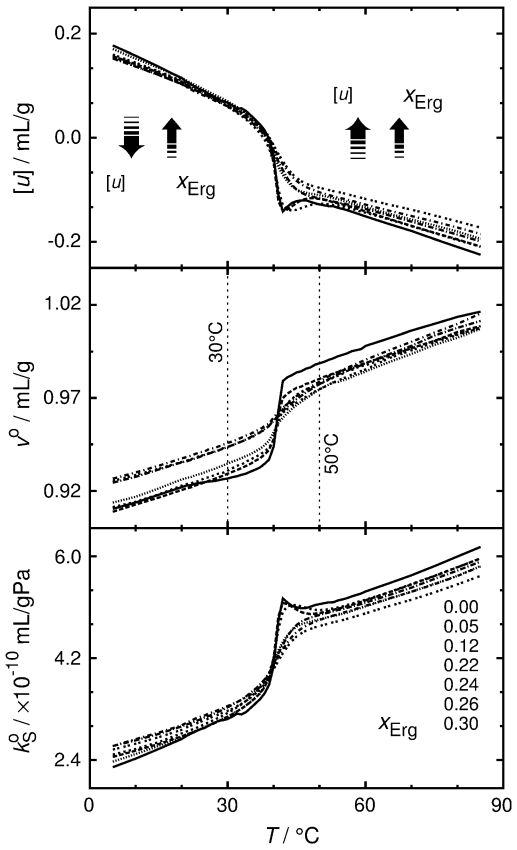

FIGURE 4 The temperature dependence of the ultrasound velocity number, $[u]$ (*upper*), the partial specific volume, v^o (*middle*), and the partial specific adiabatic compressibility, k_S^o (*lower*) of DPPC-Erg mixtures at different ergosterol molar fractions, x_{Erg}. The arrows indicate the different effects of the increasing ergosterol content on $[u]$ bellow and above the phase-transition temperature, T_m, of DPPC (41.5°C) (see text).

24, 26, and 30 mol %, and v^o of both sterols increases essentially linearly with temperature. For pure DPPC, the change of v^o at the main gel/fluid transition is ~0.04 mL/g, corresponding to an ~4% increase in the bilayer volume, which is in agreement with the value of 4.0% reported by Melchior et al. (61), and which is also very close to the 3.6% obtained by Nagle and Wilkinson (62). Here, also, as with the velocity number mentioned above, cholesterol and ergosterol have opposite effects on v^o in the gel and liquid-crystalline phases, i.e., the partial specific volume is larger below T_m and smaller above T_m for DPPC-Chol and DPPC-Erg LUVs.

As we have already mentioned, partial quantities are additive to all components of the system. In our particular case, the partial molar volume, V^o, is the sum of a membrane term, V_M^o, representing the lipid molecules of the bilayer membrane themselves, and a hydration term, V_H^o, corresponding to the hydration shell surrounding the lipid headgroups:

$$V^o = V_M^o + V_H^o. \tag{5}$$

Furthermore, for this binary lipid mixture, the membrane term, V_M^o, is given as

$$V_M^o = (1-x)V_{M,PL}^o + xV_{M,S}^o, \tag{6}$$

where $V_{M,PL}^o$ is the partial molar volume of phospholipid, $V_{M,S}^o$ is the partial molar volume of sterol, and x is the molar fraction of sterol within the binary mixture. Neglecting the smaller hydration term leads to (63)

$$V^o = V_M^o = (1-x)V_{M,PL}^o + xV_{M,S}^o, \tag{7}$$

which leads to a good estimate for the partial molar volume of the mixed membrane and can be obtained using the partial molar volume of cholesterol, $V_{M,S}^o = 325\,\text{mL/mol}$ (17), and that of DPPC, $V_{M,PL}^o = 760\,\text{mL/mol}$ (64).

Since the change in $[u]$ (~0.4 mL/mg) is around four times larger than that of v^o (~0.1 mL/mg) within the temperature interval of 5–85°C, the partial specific adiabatic compressibility, k_S^o, as determined by Eq. 4, is largely (except in the case of an offset) determined by the velocity number. The temperature dependence of k_S^o is shown in the lower portions of Figs. 3 and 4 for cholesterol and ergosterol DPPC mixtures, respectively. k_S^o for DPPC LUVs increases linearly from 2.3 mL/gPa at 5°C. Approaching the main phase transition temperature, k_S^o abruptly increases by 38% to 5.0 mL/gPa, and right after T_m, it drops by only 2%, resuming the initial increase until finally it reaches 6.2 mL/gPa at 85°C. The anomalous rise around the T_m is still remarkable at low concentrations (5 and 12 mol %) for both sterols, clearly diminishes at 22 mol %, and is fully lost for the higher sterol contents.

The adiabatic compressibility of the lipids, β_S^{lipid}, is defined as

$$\beta_S^{lipid} = -\frac{1}{v^o}\left(\frac{\partial v^o}{\partial p}\right)_S, \tag{8}$$

which is related to the partial specific adiabatic compressibility, k_S^o, by

$$k_S^o = v^o\beta_S^{lipid}. \tag{9}$$

β_S^{lipid} can thus be obtained directly from combined ultrasound velocity and density measurements. Fig. 5 shows the temperature dependence of β_S^{lipid} for the mixtures of DPPC with cholesterol (*left*) and ergosterol (*right*). In fact, the temperature course of β_S^{lipid} is essentially a copy of the shape of $k_S^o(T)$ depicted in Figs. 3 and 4, as Eq. 9 implies, including the anomalous peak at the main phase transition. For pure DPPC, β_S^{lipid}

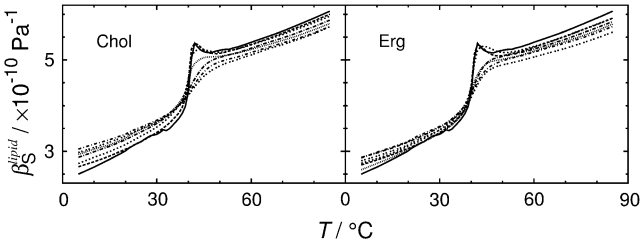

FIGURE 5 The temperature dependence of the adiabatic compressibility coefficient, β_S^{lipid}, of DPPC LUVs at various cholesterol (*left*) and ergosterol (*right*) molar fractions.

reaches 2.5×10^{-10} Pa^{-1} and 6.1×10^{-10} Pa^{-1} at 5°C and 85°C, respectively. The value for β_S^{lipid} of 3.4×10^{-10} Pa^{-1} at 30°C is in good agreement with $\beta_S^{lipid} = 3.5 \times 10^{-10}$ Pa^{-1} obtained by Mitaku and co-workers (53), but 5.2×10^{-10} Pa^{-1} at 50°C is higher compared to the literature value of 4.6×10^{-10} Pa^{-1}, which might be due to different vesicle preparations (LUV in our study and MLV in that of Mitaku et al. (53)). Similarly, for k_S^o, the anomalous increase of β_S^{lipid} around T_m is still significant at 5 and 12 mol % of both sterols, markedly declines at 22 mol %, and vanishes at higher cholesterol and ergosterol content.

Differential effects of cholesterol and ergosterol in the gel and liquid-crystalline phase of DPPC on v^o and β_S^{lipid} are shown in Fig. 6 at 30°C (gel phase) and 50°C (liquid-crystalline phase). In fact, below the T_m for pure DPPC, v^o as well as β_S^{lipid} rise with increasing sterol concentration, reflecting the ability of both sterols to decrease the conformational order of the lipid bilayer. On the other hand, both v^o and β_S^{lipid} decrease in the fluid-like phase due to the condensing effect both sterols impose above the T_m of DPPC. As already pointed out, the relative change of v^o at the main phase transition of DPPC LUV matches well with published data (61,62), and the same is also valid for the absolute values of v^o for DPPC containing cholesterol, which do not differ by >2% from literature values (61,63). v^o at 50°C decreases more or less linearly, and similarly, with increasing sterol concentration for both sterol systems. For $T = 30$°C, an abrupt increase of v^o occurs around 24 mol % for both sterols. A similar behavior was obtained by Melchior et al. (61) for DPPC-Chol mixtures. In general, the influence of ergosterol on v^o is comparable to that of cholesterol, and the cholesterol effect on the volumetric data is similar to that shown for DMPC-cholesterol mixtures (35).

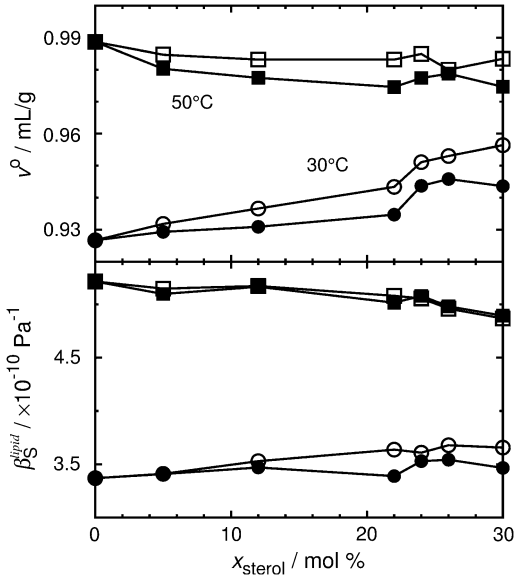

FIGURE 6 The dependence of the partial specific volume v^o (*upper*) and the adiabatic compressibility coefficient of the lipids β_S^{lipid} (*lower*) on different sterol (cholesterol and ergosterol) molar fractions below (30°C) and above (50°C) the main phase transition temperature of DPPC. (*Open symbols*) cholesterol; (*solid symbols*) ergosterol; (*squares*) 30°C; and (*circles*) 50°C.

The sterol concentration dependence of the adiabatic compressibility, β_S^{lipid}, is shown in Fig. 6 as well. In this thermodynamic parameter also, differences for the two sterols are marginal, and $\beta_S^{lipid}(x_{sterol})$ slightly increases or decreases at 50°C and 30°C, respectively. To reveal whether critical-like volume fluctuations exist at the main transition and in the l_o-l_d critical point region, isothermal compressibility data of the lipid systems have to be determined as well.

Lipid bilayer volume fluctuations

As stated above, lipid bilayer thermotropic main phase transitions are considered to be of a weak first order, i.e., they show typical features of first-order phase transitions, such as abrupt changes in specific volume or a peak in the enthalpy and entropy, but also significant fluctuations in volume and lamellar *d*-spacing, which are typical for a second-order phase transition. The isothermal compressibility, K_T, is directly proportional to the volume fluctuations of the system (65,66). In a system exhibiting a first-order transition, K_T diverges at the phase transition temperature, whereas it exhibits a power-law behavior ($K_T \propto |T - T_c|^{-\gamma}$), with a particular critical exponent ($\gamma = 1.24$ for 3D systems) in the critical-point region of a second-order phase transition (67,68). By the ultrasound velocity and density measurements, however, only the adiabatic compressibility, K_S, can be determined (see Eqs. 1 and 4). The isothermal compressibility can be calculated as (66)

$$K_T = K_S \frac{C_p}{C_V}, \tag{10}$$

where C_p and C_V are the heat capacities at constant pressure and volume, respectively, which, using Maxwell relations, can also be expressed as

$$K_T = K_S + \frac{T}{C_p}\left(\frac{\partial V}{\partial T}\right)_p^2 = K_S + \frac{TE^2}{C_p}, \tag{11}$$

with the thermal expansion $E = (\partial V/\partial T)_p$. Hence, the isothermal compressibility can be obtained from the adiabatic compressibility when the thermal expansion and the heat capacity data are available. Differentiating Eq. 11 yields the exact differential of K_T, dK_T, which is given as

$$dK_T = dK_S + \frac{E^2}{C_p}dT + 2\frac{TE}{C_p}dE - \frac{TE^2}{C_p^2}dC_p. \tag{12}$$

For convenience, Eq. 11 is adapted—through Eq. 12—by thermodynamic treatment to a form where the corresponding partial specific quantities are taken (69):

$$k_T^o = k_S^o + \frac{T\alpha_0^2}{\rho_0 c_{p,0}}\left(2\frac{e^o}{\alpha_0} - \frac{C_p^o}{\rho_0 c_{p,0}}\right), \tag{13}$$

where k_T^o is the partial specific isothermal compressibility, α_0 ($\alpha = E/V$) and $c_{p,0}$ are the thermal expansion coefficient and the specific heat capacity of the solvent, respectively; and e^o and C_p^o are the partial specific expansivity and the partial specific heat capacity of the lipid, respectively. The latter is given by Privalov (70):

$$C_p^o = \frac{\Delta C_p}{m} + \frac{v^o}{v_0^o} c_{p,0}, \tag{14}$$

where m is the mass of the solute.

The corresponding isothermal compressibility of the lipid, $\beta_T^{lipid} = k_T^o/v^o$ (please note that β_T^{lipid} differs from partial specific isothermal compressibility coefficient, β_T^o, which is defined as $\beta_T^o = 1/M(\partial\beta_T/\partial n) = (k_T^o - \beta_T v^o)/V$, can be obtained from Eq. 13 and is given as

$$\beta_T^{lipid} = \beta_S^{lipid} + \frac{T\alpha_0^2}{v^o \rho_0 c_{p,0}} \left(2\frac{e^o}{\alpha_0} - \frac{C_p^o}{\rho_0 c_{p,0}} \right). \tag{15}$$

For simplification, we denote the second and third terms in Eq. 15 as β_e^{lipid} and β_C^{lipid}, respectively:

$$\beta_T^{lipid} = \beta_S^{lipid} + \beta_e^{lipid} - \beta_C^{lipid}. \tag{16}$$

Hence, the isothermal compressibility coefficient, β_T^{lipid}, is given as a sum of the adiabatic compressibility, β_S^{lipid}, an expansion term, β_e^{lipid}, and a heat capacity term, β_C^{lipid}. Interestingly, as can be seen from Eqs. 13 and 15, the heat capacity term has a compensating effect, balancing that of the thermal expansion on the adiabatic compressibility.

The thermodynamic parameters C_p, K_T, and E are directly related to corresponding fluctuation parameters (65,71): 1), the variance of the square average of the enthalpy fluctuations, $\langle \Delta H^2 \rangle$, is determined by the heat capacity, C_p, of the system; 2), the square average of the volume fluctuations, $\langle \Delta V^2 \rangle$, is given by the respective isothermal compressibility, K_T; and 3), the covariance between H and V, $\langle \Delta H \Delta V \rangle$, is related to the thermal expansion, E, as follows:

$$\langle \Delta H^2 \rangle = RT^2 C_p, \tag{17a}$$

$$\langle \Delta V^2 \rangle = RTK_T, \tag{17b}$$

$$\langle \Delta H \Delta V \rangle = RT^2 E. \tag{17c}$$

As seen from Eq. 17c, the thermal expansion couples contributions from the heat capacity and the isothermal compressibility.

The different compressibilities of DPPC LUVs and their different contributions are shown in Fig. 7 (α_0 and $c_{p,0}$ of water were used in Eq. 16, which vary at 25°C against the values for the buffer by ~3% and ~8%, respectively). We see that $\beta_T^{lipid} > \beta_S^{lipid}$ (as expected (see Eq. 10)) by ~10% in the whole temperature range except for the region around T_m, where β_T^{lipid} distinctly differs (that is, it increases abruptly (Fig. 7, *inset*)) due to the fact that no heat transfer between the lipid bilayer and the buffer solution is expected within a time window of the ultrasound wave period (~14 μs in our experiments) for the adiabatic compressibility. Hence, β_S^{lipid} derived by means of the ultrasound velocity measurements is not able to reveal slow relaxation processes around the T_m. In fact, a drastic slowing down of the relaxation time has been observed approaching the DPPC main phase transition (34,72) and was found to be as slow as 20–45 s in MLVs and ~3 s in LUVs. It is also interesting that the expansion term, β_e^{lipid}, appears to be the predominant one in the isothermal compressibility coefficient of lipids around the T_m, whereas β_C^{lipid} is negligible (Fig. 7). This becomes apparent when the ratios of the thermal expansion coefficients and the heat capacities of lipid and solvent are taken into account (Table 1). The ratio $C_p^o/c_{p,0}$ is smaller in both the gel and liquid phase as compared to α/α_0, but the latter ratio is one order of magnitude larger and reaches a value of ~240 at the main phase transition, whereas the former achieves ~11 only. It must also be noted that values of C_p^o for DPPC MLVs obtained at both 30°C and 50°C are somewhat higher compared to the published data (~2.4 $Jg^{-1}K^{-1}$ and ~2.3 $Jg^{-1}K^{-1}$, respectively (73)). In fact, omitting the heat capacity term of the lipid, C_p, in Eq. 15 leads to an error in β_T^{lipid} of ~2% only.

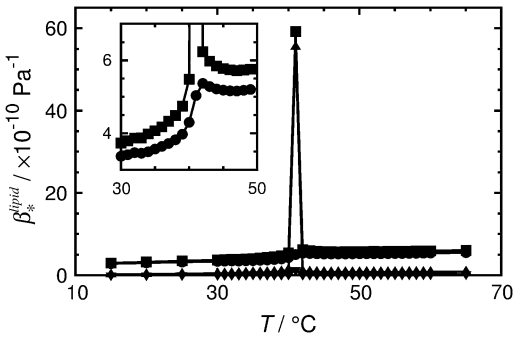

FIGURE 7 Contributions to the isothermal compressibility coefficient of the lipids in DPPC LUV, β_T^{lipid} (*squares*; see Eq. 16): the adiabatic compressibility of the lipid, β_S^{lipid} (*circles*), the thermal expansion term β_e^{lipid} (*triangles*), and the heat capacity term β_C^{lipid} (*inverted triangles*) as a function of temperature. (*Inset*) The difference between β_T^{lipid} and β_S^{lipid} in the phase transition region is depicted.

The DPPC LUV values of β_T^{lipid} in the gel phase, $3.8 \pm 0.1 \times 10^{-10}$ Pa^{-1}, and in the fluid phase, $5.8 \pm 0.2 \times 10^{-10}$ Pa^{-1}, are in good agreement with our previous data of $4.2 \pm 0.2 \times 10^{-10}$ Pa^{-1} and $5.4 \pm 0.4 \times 10^{-10}$ Pa^{-1}, respectively, determined from measurements of the partial volume as a function of the pressure (74). Regarding the phase transition region itself, peak values of β_T^{lipid} at the transition midpoint of $\sim 5.4 \pm 0.4 \times 10^{-10}$ Pa^{-1} are found. The maximum value differs from literature values available (74). This discrepancy probably arises from the different widths of the chain-melting transition (which, in turn, depends on the vesicle preparation) and the fact that the ultrasound velocity, the density, and the thermal expansion coefficient measurements were carried out with larger steps around the T_m only. The data are also in reasonable agreement with theoretical calculations of Heimburg et al. (36), which rely on a linear proportionality between the

TABLE 1 Comparison of thermal expansion coefficients of water (α_0) and DPPC LUV (α) with specific heat capacity of water ($c_{p,0}$) and partial specific heat capacity of DPPC LUVs (C_p^o) at 30, 41, and 50°C

T/°C	$\alpha_0/10^{-3}$ K^{-1}	$\alpha/10^{-3}$ K^{-1}	α/α_0	$c_{p,0}$/Jg^{-1} K^{-1}	C_p^o/Jg^{-1} K^{-1}	$C_p^o/c_{p,0}$
30	0.30	1.02 ± 0.01	3.4	4.18	5.11 ± 0.03	1.2
41	0.39	94.02 ± 0.74	241.1	4.18	45.31 ± 0.11	10.8
50	0.45	1.05 ± 0.02	2.3	4.18	4.95 ± 0.02	1.2

excess heat capacity and the volume thermal changes, which has been shown to be valid for different lipid bilayer compositions (75). Differences in absolute values might also be due to the fact that in the calculations of Heimburg et al. (36), the entire lipid solution properties, and not partial quantities, are considered.

Isothermal compressibility of DPPC-Chol and DPPC-Erg mixtures

Based on the identification of phase boundaries separating thermodynamic phases revealed by NMR and/or DSC measurements (6,7,13), phospholipid-cholesterol and phospholipid-ergosterol mixtures exhibit a liquid phase separation (into l_o and l_d phases) region (Fig. 1). In such a system, a critical point, and thus critical behavior, is expected to appear, involving a corresponding critical response in thermodynamic parameters, such as α or β_T^{lipid}. In DPPC-Chol and DPPC-Erg vesicles, a liquid-liquid critical point was found to appear at ~25 mol % (63) and ~22 mol %, respectively (see Fig. 1).

Fig. 8 (*upper*) displays the temperature dependence of the isothermal compressibility of DPPC-Chol (*left*) and DPPC-Erg (*right*) LUVs at different sterol concentrations. For both sterols, the isothermal compressibility peak at the main transition drops drastically upon addition of sterol concentrations as low as 5 mol %. The 78% decrease of β_T^{lipid} corresponds to a similar strong decrease (82%) of the thermal expansion coefficient (Fig. 2), again indicating the close relationship between the corresponding fluctuations ($\langle \Delta V^2 \rangle$ vs. $\langle \Delta H \Delta V \rangle$). At sterol concentrations >12 mol %, β_T^{lipid} is close to β_S^{lipid} in the whole temperature range covered. For the critical concentration of 22 mol % ergosterol, no significant changes in β_T^{lipid} are visible in the critical point region. The same holds true for the shape of $\alpha(T)$, which also does not exhibit any marked changes near the critical temperature (Fig. 2).

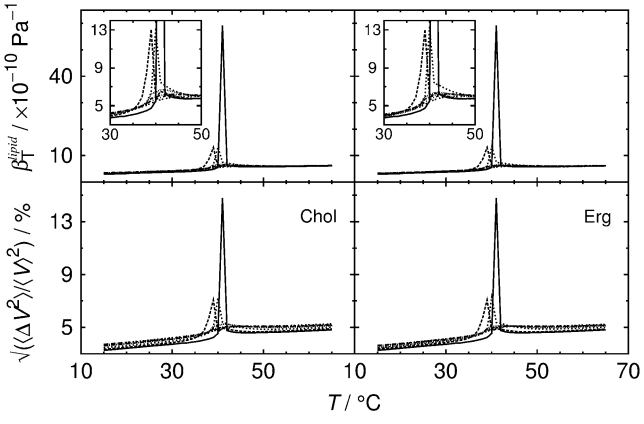

FIGURE 8 Temperature dependence of the isothermal compressibility coefficient of the lipids β_T^{lipid} (*upper*) and the calculated relative volume fluctuations (*lower*) for DPPC-sterol mixtures at different cholesterol molar fractions, x_{Chol} (*left*), and ergosterol molar fractions, x_{Erg} (*right*).

In fact, NMR data of binary phospholipid-sterol mixtures (76), recent MD simulations (77), and further experimental studies (5,22) suggest that the sterol-phospholipid binary mixtures can also be described as essentially homogeneous monophasic rather than consisting of coexisting macroscopic phase-separated regions. On the other hand, in cholesterol-phospholipid monolayers, shape transitions and critical shape fluctuations have been observed (78).

Assuming that the partial specific volume, v^o, is largely determined by the lipid term (see Eq. 7), i.e., v^o reflects the ''real'' volume of the lipid molecule, allows us to modify Eq. 17b and to convey the relative volume fluctuations given as

$$\sqrt{\frac{\langle \Delta V^2 \rangle}{V^2}} = \sqrt{\frac{RT\beta_T^{lipid}}{Mv^o}}. \tag{18}$$

The corresponding temperature dependencies are shown in Fig. 8 (*lower*) for the cholesterol-DPPC (*left*) and ergosterol-DPPC (*right*) mixtures. For DPPC at the main transition, the maximum value reached for relative volume fluctuations is 15%, and this value is strongly damped upon addition of both sterols. It is interesting that, within the accuracy of the measurements, no significant differences are observed for the two different sterols.

Fig. 9 depicts the sterol concentration dependence of β_T^{lipid} (*open symbols*, cholesterol; *solid symbols*, ergosterol) in DPPC mixtures in the ordered (30°C, *bottom curve*) and fluid (50°C, *top curve*) phase. At 30°C, the isothermal compressibility rises in a manner similar to that of the adiabatic compressibility (Fig. 6 *lower*, *bottom curve*) which increases with increasing sterol concentration, reflecting the disordering effect sterols impose on ordered phospholipid phases. β_T^{lipid} increases slightly with increasing sterol concentration at 50°C as well, whereas β_S^{lipid} seems to decrease slightly (Fig. 6).

CONCLUSIONS

We have used methods of molecular acoustics (ultrasound velocimetry and densimetry) and calorimetries (differential scanning calorimetry and pressure perturbation calorimetry)

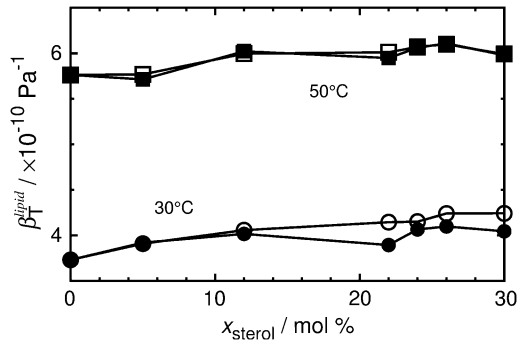

FIGURE 9 Dependence of the isothermal compressibility coefficient of the lipids, β_T^{lipid}, on the different sterol molar fractions below (30°C) and above (50°C) the main phase transition temperature of DPPC. (*Open symbols*) cholesterol; (*solid symbols*) ergosterol; (*squares*) 30°C; and (*circles*) 50°C.

to determine the isothermal compressibility coefficient and volume fluctuations of DPPC-sterol (sterols used were cholesterol and ergosterol) bilayer membranes in their different phases and at the thermotropic phase transitions exhibited by these mixtures. A particular focus was on the influence of the differential structural properties of the two sterols on the thermodynamic properties of lipid bilayers, and on the nature of the critical point region by determining thermodynamic fluctuation parameters. To the best of our knowledge, this is the first study in which such a multiprobe approach has been applied to lipid systems. Recently, we used a similar approach to study the thermodynamics of protein aggregation and fibrillization (79,80).

In pure DPPC LUVs, the isothermal compressibility coefficient has been found to be $3.8 \pm 0.1 \times 10^{-10}$ Pa^{-1} and $5.8 \pm 0.2 \times 10^{-10}$ Pa^{-1} in the gel and fluid phases, respectively. These values are ~10% higher than the corresponding adiabatic compressibility data. Based on our results, we have not found any marked difference in the effect of the different sterols (cholesterol and ergosterol) on the various thermodynamic properties studied, namely, the partial specific volume, the adiabatic and isothermal compressibility, and the volume fluctuations. Such behavior is in contrast to the distinct structural and dynamical differences the two sterols exhibit when incorporated into lipid bilayers, as revealed by our spectroscopic studies and those of others (21,31,32), where it has been shown that ergosterol orders DPPC chains more effectively than cholesterol. However, as revealed by the phase diagram shown in Fig. 1, ergosterol is more effective than cholesterol in promoting l_o-phase domains in DPPC bilayers, i.e., it is less effective in promoting lateral packing order in the liquid-like phase.

Significant differences in β_T^{lipid} and β_S^{lipid} are seen in the solid and fluid phases of the lipid bilayer, as the solvent and lipid membranes are adiabatically uncoupled in the MHz region by the ultrasound experiment. These differences become dramatic in the gel-to-fluid transition region, indicating a significant degree of slow relaxational processes in the microsecond time range in the transition region. Maximum values of 15% for relative volume fluctuations are reached for DPPC at the main transition, but these values are strongly damped upon addition of both sterols. Within the accuracy of the measurements, no significant differences are observed for the two sterols.

As revealed by detailed measurements of the temperature and concentration dependence of the isothermal compressibility and thermal expansion coefficient of the DPPC-sterol system, our data show no evidence for the existence of a typical critical point phenomenon in the concentration and temperature range where a critical point in the DPPC-sterol phase diagram is expected to appear. Hence, on a macroscopic level, it seems more appropriate to describe the sterol-phospholipid binary mixture in the $l_o + l_d$ coexistence region as a largely homogeneous phase, in accordance with earlier suggestions (5,76,77), rather than as macroscopically separated coexisting phases. Conversely, in ternary phospholipid-sterol mixtures, macroscopic phase separation is clearly observed (22,24,25). As the width of the transition peak in thermodynamic functions such as C_p, α, and β_T^{lipid} is related to the correlation length of the corresponding fluctuation parameters (or domain sizes), we can conclude that marked enthalpy and volume fluctuations are largely absent in the DPPC-sterol mixtures in their critical point region also, again pointing to the absence of macroscopic phase separation phenomena in these systems. Nanoscopic domains seem to be a more appropriate description of the lateral organization of these systems. Disordered superlatticelike domains might exist at critical concentrations of 20–22.2 mol % as well (81). Such small-domain systems are expected to exhibit additional phenomena, such as a marked entropy of mixing with other domains, an increased edge energy related to the line tension between domains, a spontaneous curvature, and a smaller lifetime, connected to a more rapid exchange of lipid molecules between domains. Such small-domain dimensions with these properties and limited lifetimes seem to be also typical of raftlike l_o domains in cell membranes (7,82). Hence, these cholesterol-sterol systems may also serve as valuable model systems for studies of such cell membrane domains.

Financial support from the Deutsche Forschungsgemeinschaft, the Fonds der Chemischen Industrie, and the country Northrhine Westfalia and the European Union (Europäischer Fonds für regionale Entwicklung) is gratefully acknowledged.

REFERENCES

1. Demel, R. A., and B. De Kruyff. 1976. The function of sterols in membranes. *Biochim. Biophys. Acta.* 57:109–132.
2. Bloom, M., and O. G. Mouritsen. 1988. The evolution of membranes. *Can. J. Chem.* 66:706–712.
3. Yeagle, P. L. 1985. Cholesterol and the cell membrane. *Biochim. Biophys. Acta.* 822:267–287.
4. Mouritsen, O. G., and M. J. Zuckermann. 2004. What's so special about cholesterol? *Lipids.* 39:1101–1113.

5. Heerklotz, H., and A. Tsamaloukas. 2006. Gradual change or phase transition: characterizing fluid lipid-cholesterol membranes on the basis of thermal volume changes. *Biophys. J.* 91:600–607.
6. Hsueh, Y.-W., K. Gilbert, C. Trandum, M. Zuckermann, and J. Thewalt. 2005. The effect of ergosterol on dipalmitoylphosphatidylcholine bilayers: a deuterium NMR and calorimetric study. *Biophys. J.* 88:1799–1808.
7. Hsueh, Y. W., M. T. Chen, P. J. Patty, C. Code, J. Cheng, B. J. Frisken, M. Zuckermann, and J. Thewalt. 2007. Ergosterol in POPC membranes: physical properties and comparison with structurally similar sterols. *Biophys. J.* 92:1606–1615.
8. Mannock, D. A., R. N. A. H. Lewis, and R. N. McElhaney. 2006. Comparative calorimetric and spectroscopic studies of the effects of lanosterol and cholesterol on the thermotropic phase behavior and organization of dipalmitoyl-phosphatidylcholine bilayer membranes. *Biophys. J.* 91:3327–3340.
9. Bacia, K., P. Schwille, and T. Kurzchalia. 2005. Sterol structure determines the separation of phases and the curvature of the liquid-ordered phase in model membranes. *Proc. Natl. Acad. Sci. USA.* 102: 3272–3277.
10. McMullen, T. P. W., and R. N. McElhaney. 1996. Physical studies of cholesterol-phospholipid interactions. *Curr. Opin. Colloid Interface Sci.* 1:83–90.
11. Mabrey, S., P. L. Mateo, and J. M. Sturtevant. 1978. High-sensitivity scanning calorimetric study of mixtures of cholesterol with dimyristoyl- and dipalmitoylphosphatidylcholines. *Biochemistry.* 17:2464–2468.
12. Scheidt, H. A., D. Huster, and K. Gawrisch. 2005. Diffusion of cholesterol and its precursors in lipid membranes studied by ^{1}H pulsed field gradient magic angle spinning NMR. *Biophys. J.* 89:2504–2512.
13. Vist, M. R., and J. H. Davis. 1990. Phase equilibria of cholesterol/dipalmitoylphosphatidylcholine mixtures: ^{2}H nuclear magnetic resonance and differential scanning calorimetry. *Biochemistry.* 29:451–464.
14. Tierney, K. J., D. E. Block, and M. L. Longo. 2005. Elasticity and phase behavior of DPPC membrane modulated by cholesterol, ergosterol, and ethanol. *Biophys. J.* 89:2481–2493.
15. Bernsdorff, C., A. Wolf, R. Winter, and E. Gratton. 1997. Effect of hydrostatic pressure on water penetration and rotational dynamics in phospholipid-cholesterol bilayers. *Biophys. J.* 72:1264–1277.
16. Bernsdorff, C., R. Winter, T. L. Hazlett, and E. Gratton. 1995. Influence of cholesterol and β-sitosterol on the dynamic behaviour of DPPC as detected by TMA-DPH and PyrPC fluorescence: a fluorescence lifetime distribution and time-resolved anisotropy study. *Ber. Bunsenges. Phys. Chem.* 99:1479–1488.
17. Sankaram, M. B., and T. E. Thompson. 1990. Modulation of phospholipid acyl chain order by cholesterol. A solid-state ^{2}H nuclear magnetic resonance study. *Biochemistry.* 29:10676–10684.
18. Ipsen, J. H., O. G. Mouritsen, and M. Bloom. 1990. Relationships between lipid membrane area, hydrophobic thickness, and acyl-chain orientational order. The effects of cholesterol. *Biophys. J.* 57:405–412.
19. Smondyrev, A. M., and M. L. Berkowitz. 2001. Molecular dynamics simulation of the structure of dimyristoylphosphatidylcholine bilayers with cholesterol, ergosterol, and lanosterol. *Biophys. J.* 80:1649–1658.
20. Estep, T. N., D. B. Mountcastle, R. L. Biltonen, and T. E. Thompson. 1978. Studies on the anomalous thermotropic behavior of aqueous dispersions of dipalmitoylphosphatidylcholine-cholesterol mixtures. *Biochemistry.* 17:1984–1989.
21. Bernsdorff, C., and R. Winter. 2003. Differential properties of the sterols cholesterol, ergosterol, β-sitosterol, *trans*-7-dehydrocholesterol, stigmasterol and lanosterol on DPPC bilayer order. *J. Phys. Chem. B.* 107:10658–10664.
22. Veatch, S. L., and S. L. Keller. 2003. Separation of liquid phases in giant vesicles of ternary mixtures of phospholipids and cholesterol. *Biophys. J.* 85:3074–3083.
23. Zuckermann, M. J., J. H. Ipsen, L. Miao, O. G. Mouritsen, M. Nielsen, J. Polson, J. Thewalt, I. Vattulainen, and H. Zhu. 2004. Modeling lipid-sterol bilayers: applications to structural evolution, lateral diffusion, and rafts. *Methods Enzymol.* 383:198–229.
24. Nicolini, C., J. Kraineva, M. Khurana, N. Periasamy, S. Funari, and R. Winter. 2006. Temperature and pressure effects on structural and conformational properties of POPC/SM/cholesterol model raft mixtures: a FT-IR, SAXS, DSC, PPC and laurdan fluorescence spectroscopy study. *Biochim. Biophys. Acta.* 1758:248–258.
25. Nicolini, C., J. Baranski, S. Schlummer, J. Palomo, M. L. Burgues, M. Kahms, J. Kuhlmann, S. Sanchez, E. Gratton, H. Waldmann, and R. Winter. 2006. Visualizing association of N-Ras in lipid microdomains: influence of domain structure and interfacial adsorption. *J. Am. Chem. Soc.* 12:192–201.
26. Henriksen, J., A. C. Rowat, E. Brief, Y. W. Hsueh, J. L. Thewalt, M. J. Zuckermann, and J. H. Ipsen. 2006. Universal behavior of membranes with sterols. *Biophys. J.* 90:1639–1649.
27. Xu, X., R. Bittman, G. Duportail, D. Heissler, C. Vilcheze, and E. London. 2001. Effect of the structure of natural sterols and sphingolipids on the formation of ordered sphingolipid/sterol domains (rafts). Comparison of cholesterol to plant, fungal, and disease-associated sterols and comparison of sphingomyelin, cerebrosides, and ceramide. *J. Biol. Chem.* 276:33540–33546.
28. McMullen, T. P. W., R. N. A. H. Lewis, and R. N. McElhaney. 2004. Cholesterol–phospholipid interactions, the liquid-ordered phase and lipid rafts in model and biological membranes. *Curr. Opin. Colloid Interface Sci.* 8:459–468.
29. Ipsen, J. H., O. G. Mouritsen, H. Wennerström, and M. J. Zuckermann. 1987. Phase equilibria in the phosphatidylcholine-cholesterol system. *Biochim. Biophys. Acta.* 905:162–172.
30. Mouritsen, O. G., and K. Jørgensen. 1994. Dynamical order and disorder in lipid bilayers. *Chem. Phys. Lipids.* 73:3–25.
31. Urbina, J. A., S. Pekerar, H. B. Le, J. Patterson, B. Montez, and E. Oldfield. 1995. Molecular order and dynamics of phosphatidylcholine bilayer membranes in the presence of cholesterol, ergosterol and lanosterol: a comparative study using ^{2}H-, ^{13}C- and ^{31}P-NMR spectroscopy. *Biochim. Biophys. Acta.* 1238:163–176.
32. Endress, E., S. Bayerl, D. Prechtel, C. Maier, R. Merkel, and T. M. Bayerl. 2002. The effect of cholesterol, lanosterol, and ergosterol on lecithin bilayer mechanical properties at molecular and microscopic dimensions: a solid-state NMR and micropipet study. *Langmuir.* 18:3293–3299.
33. Pencer, J., M. P. Nieh, T. A. Harroun, S. Krueger, C. Adams, and J. Katsaras. 2005. Bilayer thickness and thermal response of dimyristoylphosphatidylcholine unilamellar vesicles containing cholesterol, ergosterol and lanosterol: a small-angle neutron scattering study. *Biochim. Biophys. Acta.* 1720:84–91.
34. van Osdol, W. W., M. L. Johnson, Q. Ye, and R. L. Biltonen. 1991. Relaxation dynamics of the gel to liquid-crystalline transition of phosphatidylcholine bilayers. Effects of chainlength and vesicle size. *Biophys. J.* 59:775–785.
35. Halstenberg, S., T. Heimburg, T. Hianik, U. Kaatze, and R. Krivanek. 1998. Cholesterol-induced variations in the volume and enthalpy fluctuations of lipid bilayers. *Biophys. J.* 75:264–271.
36. Heimburg, T. 1998. Mechanical aspects of membrane thermodynamics. Estimation of the mechanical properties of lipid membranes close to the chain melting transition from calorimetry. *Biochim. Biophys. Acta.* 1415: 147–162.
37. Heimburg, T. 2007. Thermal Biophysics of Membranes. Wiley-VCH, Weinheim, Germany.
38. Halstenberg, S., W. Schrader, P. Das, J. K. Bhattacharjee, and U. Kaatze. 2003. Critical fluctuations in the domain structure of lipid membranes. *J. Chem. Phys.* 118:5683–5691.
39. Mitaku, S., T. Jippo, and R. Kataoka. 1983. Thermodynamic properties of the lipid bilayer transition: Pseudocritical phenomena. *Biophys. J.* 42:137–144.
40. Nagle, J. F. 1980. Theory of the main lipid bilayer phase transition. *Annu. Rev. Phys. Chem.* 31:157–196.
41. Cevc, G., and D. Marsh. 1987. Phospholipid bilayers. John Wiley & Sons, New York.
42. MacDonald, R. C., R. I. MacDonald, B. P. M. Menco, K. Takeshita, N. K. Subbarao, and L.-R. Hu. 1991. Small-volume extrusion apparatus

for preparation of large unilamellar vesicles. *Biochim. Biophys. Acta.* 1061:297–303.

43. Eggers, F., and T. Funk. 1973. Ultrasonic measurements with milliliter liquid sample in the 0.5–100 MHz range. *Rev. Sci. Instrum.* 44:969–978.
44. Eggers, F., and K. Kustin. 1969. Ultrasonic methods. *Methods Enzymol.* 16:55–80.
45. Stuehr, J., and E. Yeager. 1965. The propagation of sound in electrolytic solutions. *In* Physical Acoustics. Vol. 2A. W. P. Mason. editor. Academic Press, New York.
46. Kratky, O., H. Leopold, and H. Stabinger. 1973. The determination of partial specific volume of protein by the mechanical oscillator technique. *Methods Enzymol.* 27:98–110.
47. Heerklotz, H., and J. Seelig. 2002. Application of pressure perturbation calorimetry to lipid bilayers. *Biophys. J.* 82:1445–1452.
48. Ravindra, R., and R. Winter. 2003. Pressure perturbation calorimetric studies of the solvation properties and the thermal unfolding of proteins in solution. *Z. Phys. Chem.* 217:1221–1243.
49. Dzwolak, W., R. Ravindra, J. Lendermann, and R. Winter. 2003. Aggregation of bovine insulin probed by DSC/PPC calorimetry and FTIR spectroscopy. *Biochemistry.* 42:11347–11355.
50. Ravindra, R., C. Royer, and R. Winter. 2004. Pressure perturbation calorimetric studies of the solvation properties and the thermal unfolding of staphylococcal nuclease. *Phys. Chem. Chem. Phys.* 6:1952–1961.
51. Ravindra, R., and R. Winter. 2004. Pressure perturbation calorimetry: a new technique provides surprising results on the effects of co-solvents on protein solvation and unfolding behaviour. *ChemPhysChem.* 5:566–571.
52. Mitra, L., N. Smolin, R. Ravindra, C. Royer, and R. Winter. 2006. Pressure perturbation calorimetric studies of the solvation properties and the thermal unfolding of proteins in solution. Experiments and theoretical interpretation. *Phys. Chem. Chem. Phys.* 8:1249–1265.
53. Mitaku, S., A. Ikegami, and A. Sakanishi. 1978. Ultrasonic studies of lipid bilayer. Phase transition in synthetic phosphatidylcholine liposomes. *Biophys. Chem.* 8:295–304.
54. Kharakoz, D. P., A. Colotto, K. Loher, and P. Laggner. 1993. Fluid-gel interphase line tension and density fluctuations in dipalmitoylphosphatidylcholine multilamellar vesicles: an ultrasonic study. *J. Phys. Chem.* 97:9844–9851.
55. Schrader, W., H. Ebel, P. Grabitz, E. Hanke, T. Heimburg, M. Hoeckel, M. Kahle, F. Wente, and U. Kaatze. 2002. Compressibility of lipid mixtures studied by calorimetry and ultrasonic velocity measurements. *J. Phys. Chem.* 106:6581–6586.
56. Mitaku, S., and T. Data. 1982. Anomalies of nanosecond ultrasonic relaxation in the lipid bilayer transition. *Biochim. Biophys. Acta.* 688: 411–421.
57. Sakanishi, A., S. Mitaku, and A. Ikegami. 1979. Stabilizing effect of cholesterol on phosphatidylcholine vesicles observed by ultrasonic velocity measurement. *Biochemistry.* 18:2636–2642.
58. van Osdol, W. W., R. L. Biltonen, and M. L. Johnson. 1989. Measuring the kinetics of membrane phase transition. *J. Bioenerg. Biophys. Methods.* 20:1–46.
59. Heimburg, T., and D. Marsh. 1996. Thermodynamics of the interaction of proteins with lipid membranes. *In* Biological Membranes: A Molecular Perspective from Computation and Experiment. K. M. Merz and B. Roux, editors. Birkhauser, Boston. 405–462.
60. Kaatze, U., B. O'Driscoll, E. Hanke, M. Jäger, and V. Buckin. 2006. Ultrasonic calorimetry of membranes. *Pharm. Technol. Eur.* 47:1–5.
61. Melchior, D. L., F. J. Scavitto, and J. M. Steim. 1980. Dilatometry of dipalmitoyllecithin-cholesterol bilayers. *Biochemistry.* 19:4828–4834.
62. Nagle, J. F., and D. A. Wilkinson. 1978. Lecithin bilayers. Density measurements and molecular interactions. *Biophys. J.* 23:159–175.
63. Greenwood, A. I., S. Tristram-Nagle, and J. F. Nagle. 2006. Partial molecular volumes of lipids and cholesterol. *Chem. Phys. Lipids.* 143: 1–10.
64. Nagle, J. F., and S. Tristram-Nagle. 2000. Structure of lipid bilayers. *Biochim. Biophys. Acta.* 1469:159–195.
65. Hill, T. L. 1960. An Introduction to Statistical Thermodynamics. Dover, New York.
66. Wilson, A. H. 1957. Thermodynamics and Statistical Mechanics. Cambridge University Press, Cambridge, UK.
67. Stanley, H. E. 1971. Introduction to Phase Transitions and Critical Phenomena. Oxford University Press, New York.
68. Winter, R., A. Gabke, C. Czeslik, and P. Pfeifer. 1999. Power-law fluctuations in phase-separated lipid membranes. *Phys. Rev. E Stat. Phys. Plasmas Fluids Relat. Interdiscip. Topics.* 60:7354–7359.
69. Chalikian, T. V. 2003. Volumetric properties of proteins. *Annu. Rev. Biophys. Biomol. Struct.* 32:207–235.
70. Privalov, P. L. 1980. Scanning microcalorimeters for studying macromolecules. *Pure Appl. Chem.* 52:479–497.
71. Cooper, A. 1984. Protein fluctuations and the thermodynamic uncertainty principle. *Prog. Biophys. Mol. Biol.* 44:181–214.
72. Grabitz, P., V. P. Ivanova, and T. Heimburg. 2002. Relaxation kinetics of lipid membranes and its relation to the heat capacity. *Biophys. J.* 82:299–309.
73. Blume, A. 1983. Apparent molar heat capacities of phospholipids in aqueous dispersion. Effects of chain length and head group structure. *Biochemistry.* 22:5436–5442.
74. Seemann, H., and R. Winter. 2003. Volumetric properties, compressibilities and volume fluctuations in phospholipid-cholesterol bilayers. *Z. Phys. Chem.* 217:831–846.
75. Edel, H., P. Grabitz, and T. Heimburg. 2001. Enthalpy and volume changes in lipid membranes. I. The proportionality of heat and volume changes in the lipid melting transition and its implication for the elastic constants. *J. Phys. Chem. B.* 105:7353–7360.
76. McConnell, H., and A. Radhakishnan. 2006. Theory of the deuterium NMR of sterol-phospholipid membrane. *Proc. Natl. Acad. Sci. USA.* 103:1184–1189.
77. Pandit, S. A., G. Khelashvili, E. Jakobson, A. Grema, and H. L. Scott. 2007. Lateral organization in lipid-cholesterol mixed bilayers. *Biophys. J.* 92:440–447.
78. Rice, P. A., and H. M. McConnell. 1989. Critical shape transitions of monolayer lipid domains. *Proc. Natl. Acad. Sci. USA.* 86:6445–6448.
79. Smirnovas, V., R. Winter, T. Funck, and W. Dzwolak. 2005. Thermodynamic properties underlying the α-helix-to-β-sheet transition, aggregation and amyloidogenesis of polylysine as probed by calorimetry, densimetry and ultrasound velocimetry. *J. Phys. Chem. B.* 109: 19043–19045.
80. Smirnovas, V., R. Winter, T. Funck, and W. Dzwolak. 2006. Protein amyloidogenesis in the context of volume fluctuations: a case study on insulin. *ChemPhysChem.* 7:1046–1049.
81. Venegas, B., I. P. Sugár, and P. L.-G. Chong. 2007. Critical factors for detection of biphasic changes in membrane properties at specific sterol mole fractions for maximal superlattice formation. *J. Phys. Chem. B.* 111:5180–5192.
82. Kusumi, A., I. Koyama-Honda, and K. Suzuki. 2004. Molecular dynamics and interactions for creation of stimulation-induced stabilized rafts from small unstable steady-state rafts. *Traffic.* 5:213–230.